

RESEARCH

Open Access



# Mulberroside A mitigates intervertebral disc degeneration by inhibiting MAPK and modulating Ppar- $\gamma$ /NF- $\kappa$ B pathways

Tao Xu<sup>1</sup>, Hongqi Zhao<sup>1</sup>, Xuan Fang<sup>1</sup>, Shanxi Wang<sup>1</sup>, Jian Li<sup>2</sup>, Hua Wu<sup>1</sup>, Weihua Hu<sup>1\*</sup> and Rui Lu<sup>1,3\*</sup>

## Abstract

**Background** Intervertebral disc degeneration (IVDD) is a common spine disease with inflammation as its main pathogenesis. Mulberroside A (MA), isolated from herbal medicine, possesses anti-inflammatory characteristics in many diseases. Whereas, there is little exploration of the therapeutic potential of MA on IVDD. This study aimed at the therapeutic potential of MA on IVDD in vivo and in vitro and the mechanism involved.

**Methods** In vitro, western blotting, RT-qPCR, and immunofluorescence analysis were implemented to explore the bioactivity of MA on interleukin-1 beta (IL-1 $\beta$ )-induced inflammation nucleus pulposus cells (NPCs) isolated from Sprague-Dawley male rats. In vivo, X-ray and MRI were applied to measure the morphological changes, and histological staining and immunohistochemistry were employed to investigate the histological changes of intervertebral disc sections on puncture-induced IVDD rat models.

**Results** In vitro, MA up-regulated the expression level of anabolic-related proteins (Aggrecan and Collagen II) and decreased catabolic-related proteins (Mmp2, Mmp3, Mmp9, and Mmp13) in IL-1 $\beta$ -induced NPCs. Furthermore, MA inhibits the production of pro-inflammatory factors (Inos, Cox-2, and Il-6) stimulated by IL-1 $\beta$ . Mechanistically, MA inhibited the signal transduction of mitogen-activated protein kinase (MAPK) and nuclear factor kappa-B (NF- $\kappa$ B) pathways in IL-1 $\beta$ -induced NPCs. Moreover, MA might bind to Ppar- $\gamma$  and then suppress the NF- $\kappa$ B pathway. In vivo experiment illustrated that MA mitigates the IVDD progression in puncture-induced IVDD model. X-ray and MRI images showed MA restore the disc height and T2-weighted signal intensity after puncturing. H&E and Safranin O/ Fast Green also showed MA also alleviated morphological changes caused by acupuncture. In addition, MA reversed the expression level of Mmp13, Aggrecan, Collagen II, and Ppar- $\gamma$  induced in IVDD models.

**Conclusions** MA inhibited degenerative phenotypes in NPCs and alleviated IVDD progression via inhibiting the MAPK and NF- $\kappa$ B pathways; besides, MA suppressed the NF- $\kappa$ B pathway was attributed to activating Ppar- $\gamma$ , those supported that MA or Ppar- $\gamma$  might be a potential drug or target for IVDD.

**Keywords** Intervertebral disc degeneration, Mulberroside A, Ppar- $\gamma$ , MAPK, NF- $\kappa$ B

\*Correspondence:

Weihua Hu  
whhu@tjh.tjmu.edu.cn  
Rui Lu  
hblurui2023@whu.edu.cn

<sup>1</sup>Department of Orthopedics, Tongji Hospital, Tongji Medical College, Huazhong University of Science and Technology, Wuhan, Hubei, China

<sup>2</sup>Department of Orthopaedics, Third Hospital of Shanxi Medical University, Shanxi Bethune Hospital, Shanxi Academy of Medical Sciences, Tongji Shanxi Hospital, Taiyuan, China

<sup>3</sup>Department of Thoracic Surgery, Zhongnan Hospital of Wuhan University, Wuhan, Hubei, China



© The Author(s) 2024. **Open Access** This article is licensed under a Creative Commons Attribution-NonCommercial-NoDerivatives 4.0 International License, which permits any non-commercial use, sharing, distribution and reproduction in any medium or format, as long as you give appropriate credit to the original author(s) and the source, provide a link to the Creative Commons licence, and indicate if you modified the licensed material. You do not have permission under this licence to share adapted material derived from this article or parts of it. The images or other third party material in this article are included in the article's Creative Commons licence, unless indicated otherwise in a credit line to the material. If material is not included in the article's Creative Commons licence and your intended use is not permitted by statutory regulation or exceeds the permitted use, you will need to obtain permission directly from the copyright holder. To view a copy of this licence, visit <http://creativecommons.org/licenses/by-nc-nd/4.0/>.

## Introduction

Intervertebral disc degeneration (IVDD) is a common spinal disease that any spinal surgeon is in frequent contact with, and it is a major cause of low back pain, which seriously worsens the health-related quality of life and causes an enormous socio-economic burden [1–3]. IVDD is influenced by a variety of factors, including age, lifestyle, trauma, mechanical stress, and genetics, but, the exact mechanism of IVDD remains unclear [4–6].

The progression of IVDD is characterised by changes in cellular metabolism in the intervertebral disc microenvironment, leading to progressive structural and functional damage. Recent studies have shown that the overproduction of pro-inflammatory mediators plays a critical role in the pathological processes of IVDD, such as extracellular matrix (ECM) degradation, cell senescence, and apoptosis [7, 8]. The secretion of pro-inflammatory mediators contributes to the signaling transduction of mitogen-activated protein kinase (MAPK) and nuclear factor-kappa-B (NF- $\kappa$ B) pathways, and previous researches have reported that the above two pathways play a crucial role in the degeneration of ECM in nucleus pulposus cells (NPCs) [9, 10]. Therefore, inhibiting inflammatory response is critical for the treatment of IVDD.

Mori Cortex is one of the well-known traditional Chinese herbal medicines, which exhibits great medicinal properties in various diseases [11, 12]. Mulberroside A (MA), a natural polyhydroxylated stilbene compound extracted from Mori cortex [13], has been demonstrated to have some biological properties, including anti-hyperuricemic, anti-inflammatory, and analgesic properties [13–15]. In our previous study, MA showed the ability of down-regulate the protein generation of IL-1 $\beta$  and IL-6 via suppressing the signal transduction of MAPK and NF- $\kappa$ B pathways in chondrocytes, thereby exhibiting anti-inflammatory effects [16]. However, whether MA has an anti-inflammatory effect on IVDD remains unknown. Therefore, we used an IL-1 $\beta$ -induced NPCs to investigate the potential role of MA on IVDD in this study.

## Materials and methods

### Experimental materials and reagents

MA (HY-N0619), GW9662 (HY-16,578) and dimethyl sulfoxide (DMSO, HY-Y0320) were purchased from MedChemExpress (Monmouth Junction, NJ, USA). Recombinant rat interleukin-1 beta (IL-1 $\beta$ ) protein was purchased from R&D Systems (Minneapolis, USA).

### Animals

Sprague-Dawley (SD) rats (6 weeks old, male) were obtained from the Hubei Province Experimental Animal Centre (Wuhan, China). The study was approved by the Animal Experimentation Ethics Committee of Tongji

Hospital, Tongji Medical College, Huazhong University of Science and Technology.

### Harvest and culture of primary nucleus pulposus cells (NPCs)

The primary NPCs were obtained from the nucleus pulposus of 6w SD male rats. Briefly, nucleus pulposus tissues were harvested under sterile conditions and then incubated with 0.25% trypsin at 37 °C for 0.5 h. The samples were then digested with collagenase II at 37 °C for 3 h. After removal of collagenase II, the DMEM/F12 medium (Hyclone, USA) containing with 10% fetal bovine serum (Gibco, USA) was used to culture NPCs. The NPCs in the 1st or 2nd passages were used for the following study.

### Cell viability assessment

The viability of NPCs with different treatment were analyzed using a cell counting kit-8 (CCK-8, Boster, China) and a Calcein/PI staining assay kit (Beyotime, China). In brief, NPCs were seeded into 96-well plates, followed by the treatment with IL-1 $\beta$  (5 ng/mL) and concentration gradients of MA (20, 40, and 80  $\mu$ M) for 24 h. Afterwards, the CCK-8 reagent was added to the cells and a microplate reader (BioTek, USA) was employed to evaluate cell viability. For the Calcein/PI staining assay, a fluorescence microscope (EVOS FI AUTO, USA) was used to capture live/dead cell images, and the percentage of live cells to total cells was counted by Image J.

### Western blotting

Briefly, NPCs with different interventions were lysed on ice for 0.5 h using a lysate reagent. Afterwards, The BCA kit (Boster, China) was employed to measure the concentrations of protein samples. Cellular proteins (20  $\mu$ g) were separated by electrophoresis and transferred to a membrane. Bovine serum albumin (5%) was used to block the protein bands, which were then incubated with corresponding primary antibodies listed in Table 1 at 4 °C for 16 h, and with secondary antibodies at room temperature for 1 h. Finally, Image Lab System (Bio-Rad, USA) was used to analyse the target protein bands.

### Real time-quantitative polymerase chain reaction (RT-qPCR)

Total RNA was extracted using a TRIZOL kit (Takara Bio Inc, Japan), and cDNA was synthesized using a cDNA synthesis kit (Yeasen, China). The amplification of cDNA was performed using an RT-qPCR kit, and specific primers are listed in Table 2. The relative mRNA levels were determined using the  $2^{-\Delta\Delta C_t}$  method.

### Immunofluorescence staining

A suitable number of cells were incubated in a 24-well cell culture plate and subjected to various treatments

**Table 1** Primary antibodies for western bolt

Primary Antibody	Catalog Number	Dilution Ratio	Source
Gapdh	60004-1-Ig	1:50,000	Proteintech Group, Wuhan, Hubei, China
Aggrecan	13880-1-AP	1:1,000	Proteintech Group, Wuhan, Hubei, China
Collagen I	# 84,336	1:1,000	Cell Signaling Technology, Beverly, MA, USA
Collagen II	28459-1-AP	1:1,000	Proteintech Group, Wuhan, Hubei, China
Mmp2	66366-1-Ig	1:1000	Proteintech Group, Wuhan, Hubei, China
Mmp3	BM4074	1:500	Boster, Wuhan, Hubei, China
Mmp9	10375-2-AP	1:500	Proteintech Group, Wuhan, Hubei, China
Mmp13	18165-1-AP	1:1,000	Proteintech Group, Wuhan, Hubei, China
Cox-2	# 12,282	1:1,000	Cell Signaling Technology, Beverly, MA, USA
Inos	#13,120	1:1,000	Cell Signaling Technology, Beverly, MA, USA
Il-6	A14687	1:500	ABclonal, Wuhan, Hubei, China
Ppar-γ	A11183	1:1000	ABclonal, Wuhan, Hubei, China
p-P38	#4511	1:1,000	Cell Signaling Technology, Beverly, MA, USA
P38	#8690	1:1,000	Cell Signaling Technology, Beverly, MA, USA
p-Erk	#4377	1:1,000	Cell Signaling Technology, Beverly, MA, USA
Erk	#4695	1:1,000	Cell Signaling Technology, Beverly, MA, USA
p-Jnk	#4668	1:1,000	Cell Signaling Technology, Beverly, MA, USA
Jnk	#9252	1:1,000	Cell Signaling Technology, Beverly, MA, USA
p-P65	#3033	1:1,000	Cell Signaling Technology, Beverly, MA, USA
P65	#8242	1:1,000	Cell Signaling Technology, Beverly, MA, USA

**Table 2** Primer sequence used in the RT-qPCR experiment

Gene	Sequence
Rat-Collagen II-F	5'-CGAGGCAGACAGTACCTTG-3'
Rat-Collagen II-R	5'-TGCTCTCGATCTGGTTGTTTC-3'
Rat-Mmp13-F	5'-CAAGCAGCTCCAAGGCTAC-3'
Rat-Mmp13-R	5'-TGGCTTTTGCCAGTGTAGGT-3'
Rat-Cox-2-F	5'-CTCAGCCATGCAGCAAATCC-3'
Rat-Cox-2-R	5'-GGGTGGGCTTCAGCAGTAAT-3'
Rat-Inos-F	5'-CTATCCCCAGCCCAACAACAC-3'
Rat-Inos-R	5'-GTCACATGCAGCTTGTCCAG-3'
Rat-Gapdh-F	5'-GGTGAAGGTCGGTGTGAACG-3'
Rat-Gapdh-R	5'-CTCGCTCCTGGAAGATGGTG-3'

F: Forward; R: Reverse

after attachment. Following a rinse with Tris Buffered Saline with Tween (TBST), the cells were fixed with a fixation reagent (Servicebio, China) for 0.5 h and then permeabilized with 0.2% Triton X-100 (BioFroxx, Germany) for 0.1 h. After being blocked for 1 h, the NPCs were incubated with the primary antibodies (Mmp13, Collagen II, and p-P65, 1:200) at 4 °C for more than 16 h. Subsequently, corresponding fluorescent secondary antibodies (Boster, China) were added to the cells and incubated for 1 h away from light. The nucleus of NPCs was then stained with a DAPI solution (Boster, China) for 0.1 h. Finally, images of immunofluorescence staining were captured using a microscope.

**IVDD model generation and treatment**

According to previous study, rat IVDD models can be constructed through needle puncture to the tail disc in vivo experiments [17, 18]. A total of 18 rats were used for in vivo experiments and three intervention measures were implemented in consecutive discs in rat coccygeal (Co7/8-Co9/10) of the same individual in order to reduce errors caused by individual differences. The discs in Co7/8-Co9/10 of each rat were divided into three groups as follows: (1) The SHAM group, which received no treatment in the disc of Co7/8. (2) The IVDD group, which was punctured and injected 2 μL Phosphate Buffered Saline (PBS) in the disc of Co8/9. (3) The IVDD + MA group, which was punctured and injected with 2 μL 80 μM MA in the disc of Co9/10. After 8 weeks, radiological analysis and histological staining were performed.

**Radiological analysis**

A digital X-ray imaging system (uDR 780i, Union Imaging, China) was used to perform an X-ray on the coccygeal vertebra. Surgimap software V.2.3.2 was used to measure the disc height index (DHI) [19]. A 3.0T magnetic resonance imaging (MRI) scanner (uMR 780, union imaging, China) was employed to obtain T2-weighted MR images in the coronal (Cor) and sagittal (Sag) plane. Finally, the MRI images were analyzed using the Pfirrmann score [20].

**Statistical analysis**

All data were shown as mean ± standard deviation (SD) and analyzed using GraphPad Prism V.8 (GraphPad Software Inc., USA). The normal distribution was assessed using the Shapiro-Wilk test. One-way analysis of variance followed by Tukey post hoc test was used to analyze data between multiple experimental groups that meet the normal distribution. Otherwise, the Kruskal–Wallis test was used. The *p* value less than 0.05 was considered as statistical significance.

**Results**

**Viability of NPCs treated with IL-1 $\beta$ /MA and selection of optimal concentrations of MA**

The molecular formula of MA is in Fig. 1A. The viability of NPCs was assessed using a CCK-8 kit to determine the effects of IL-1 $\beta$  and MA. As shown in Fig. 1B, the data indicates that NPCs viability was inhibited by 160  $\mu$ M MA at 24 h ( $p < 0.05$ ), while MA at or below 80  $\mu$ M did not affect NPC viability ( $p > 0.05$ ). Furthermore, the CCK-8 and Calcein/PI staining assay demonstrated that cell viability was not affected by the administration of varying concentrations of MA and/or 5 ng/mL IL-1 $\beta$  alone or in combination for 24 h ( $p > 0.05$ ) (Fig. 1C-E). Therefore, we chose to use MA at concentrations of 20, 40, and 80  $\mu$ M for subsequent experiments.

**MA inhibited the ECM degeneration in IL-1 $\beta$ -induced NPCs**

To investigate the role of MA in ECM metabolism during the progression of IVDD, NPCs were induced with IL-1 $\beta$  (5 ng/ml) or/and MA (20, 40, and 80  $\mu$ M) for 24 h. As shown in Fig. 2A-B, IL-1 $\beta$  decreased the protein

levels of Aggrecan and Collagen II, while increasing the generation of Collagen (I) However, the degenerative effects induced by IL-1 $\beta$  were reversed by the application of 80  $\mu$ M MA. In addition, IL-1 $\beta$  upregulated the protein expression of matrix metalloproteinases (Mmps), including Mmp2, Mmp3, Mmp9, and Mmp13, whereas MA downregulated the expression of Mmps (Fig. 2C-D). Additionally, RT-qPCR analysis in Fig. 2H demonstrated that MA increased the mRNA levels of the Collagen II gene and decreased the mRNA levels of the Mmp13 gene after IL-1 $\beta$  stimulation. In Fig. 2E-G, immunofluorescence staining also showed that IL-1 $\beta$  upregulated the protein level of Mmp13 and downregulated the Collagen II, as the fluorescence intensity of Mmp13 increased and Collagen II decreased. However, MA treatment reversed the protein generation of Mmp13 and Collagen (II) Therefore, MA inhibits ECM degeneration in NPCs induced by IL-1 $\beta$ .

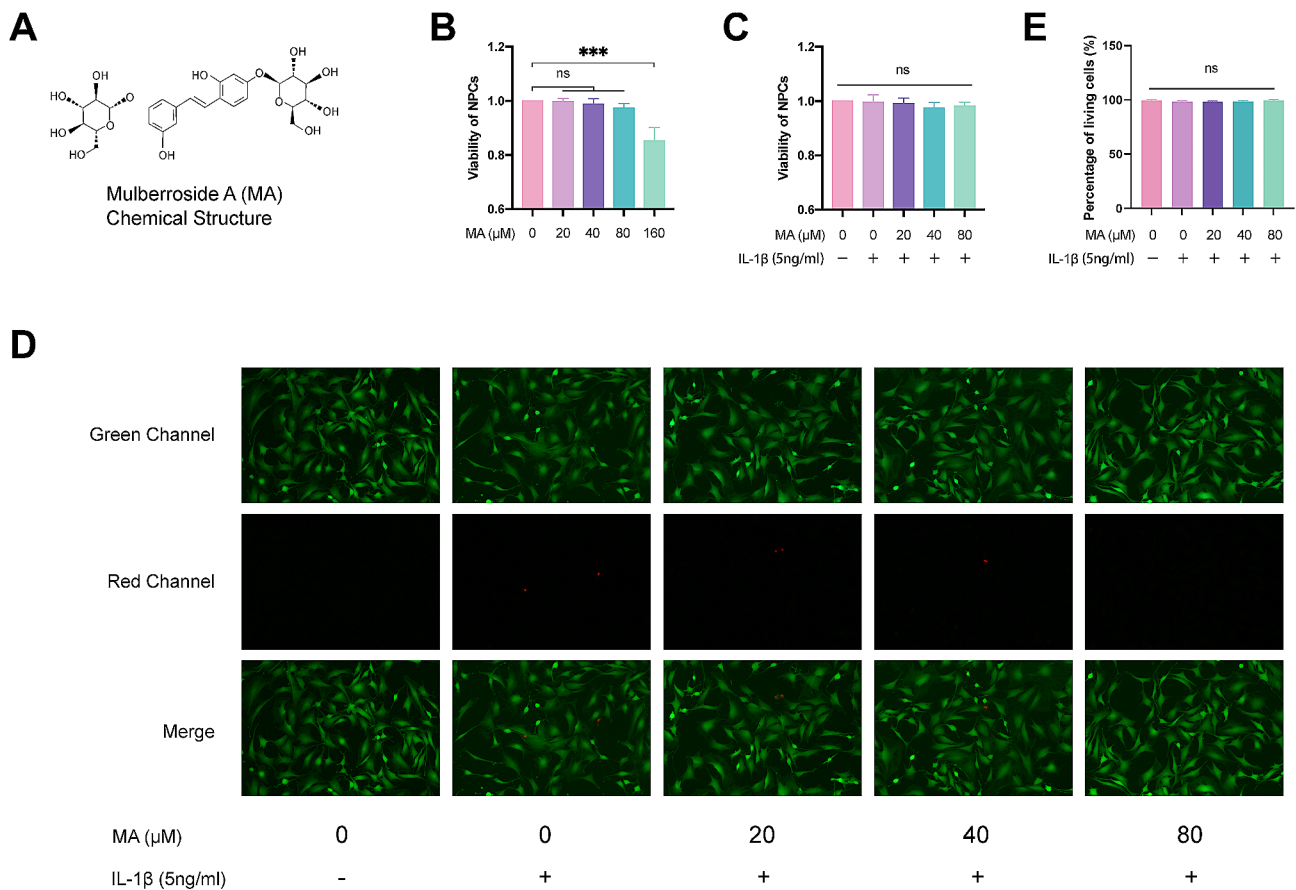


**Fig. 1** Viability of NPCs intervened with MA/IL-1 $\beta$  and choice of optimal concentrations of MA. **(A)** Chemical structure of MA. **(B)** The viability of NPCs intervened with different MA concentrations (0, 20, 40, 80, and 160  $\mu$ M) for 24 h was evaluated by a CCK-8 kit. **(C)** The viability of NPCs was intervened with IL-1 $\beta$  (5 ng/mL) alone or with different MA concentrations (20, 40, and 80  $\mu$ M) for 24 h was evaluated by a CCK-8 kit. **(D)** A Calcein /PI double staining of NPCs after intervention with IL-1 $\beta$  (5 ng/mL) alone or with different MA concentrations (20, 40, and 80  $\mu$ M) for 24 h (green, living cells; red, nucleus of dead cells). **(E)** Quantitative analysis of the percentage of living cells. Data were shown as means  $\pm$  SD,  $n = 3$ . \*\*\* $p < 0.001$ ; ns, no significant difference

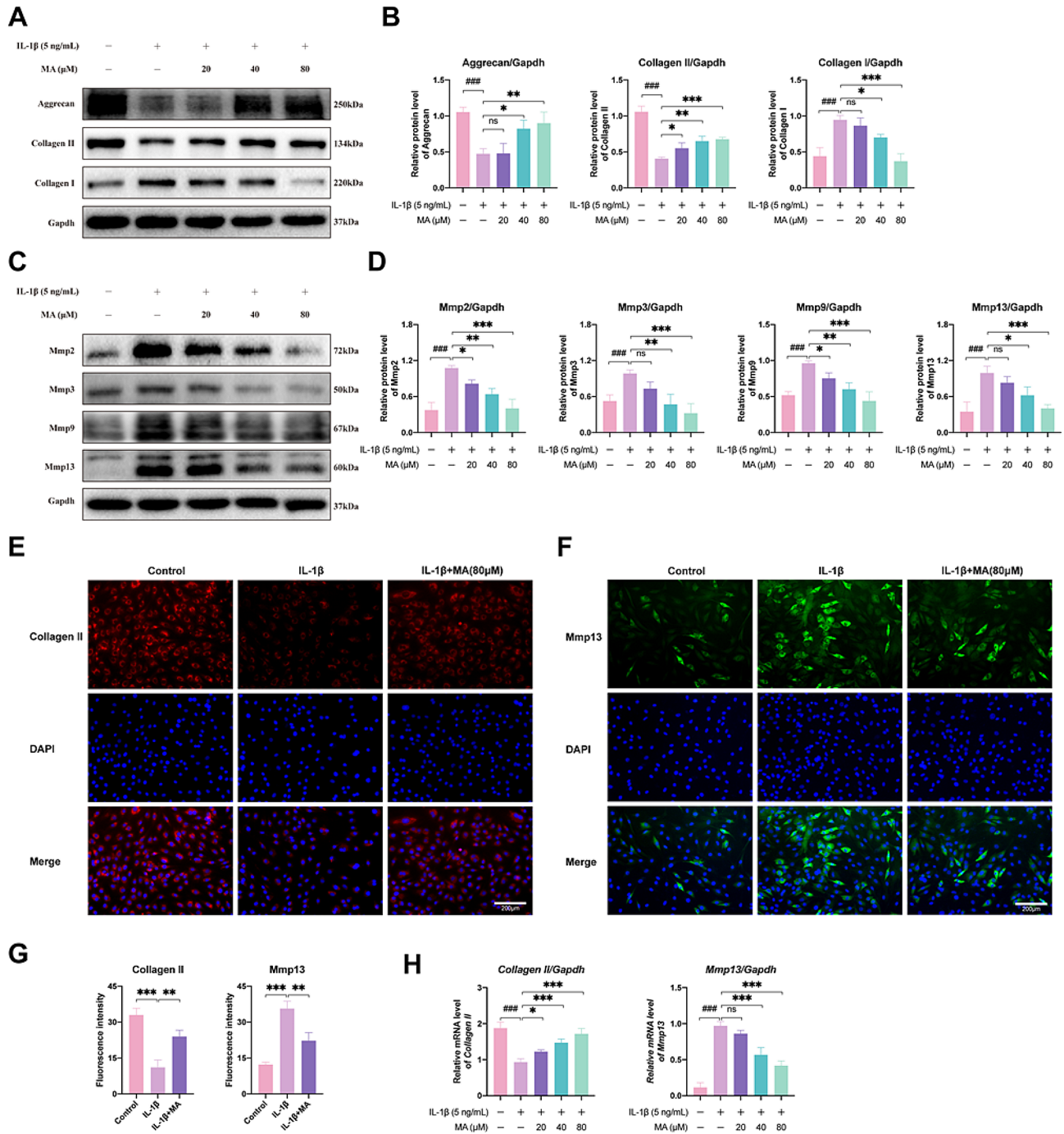


**Fig. 2** MA inhibited IL-1 $\beta$ -stimulated ECM degeneration in NPCs. **(A-D)** The expressions of anabolic-related proteins (Aggrecan, Collagen II, and Collagen I) and catabolic-related proteins (Mmp2, Mmp3, Mmp9, and Mmp13) in NPCs were analyzed with western blotting. **(E-G)** the expressions of Collagen II and Mmp13 were detected by immunofluorescence, scalebar = 200  $\mu$ m. **(H)** The mRNA expression of Collagen II and Mmp13 were analyzed by RT-qPCR. Data were shown as means  $\pm$  SD,  $n=3$ . \* $p < 0.05$ ; \*\* $p < 0.01$ ; \*\*\* $p < 0.001$ ; ns, no significant difference

### MA reduced the inflammation responses in IL-1 $\beta$ -induced NPCs

To investigate whether MA inhibited the inflammation response in NPCs induced by IL-1 $\beta$ , we detected the expression of pro-inflammatory factors, including Inos, Cox-2, and Il-6. As shown in Fig. 3A-B, we saw that IL-1 $\beta$

significantly increased the production of Inos, Cox-2, and Il-6 at the protein level. However, the upregulation of these inflammatory phenotypes was inhibited after MA treatment. In addition, similar trends in mRNA expression were observed under the same intervention conditions (Fig. 3C).

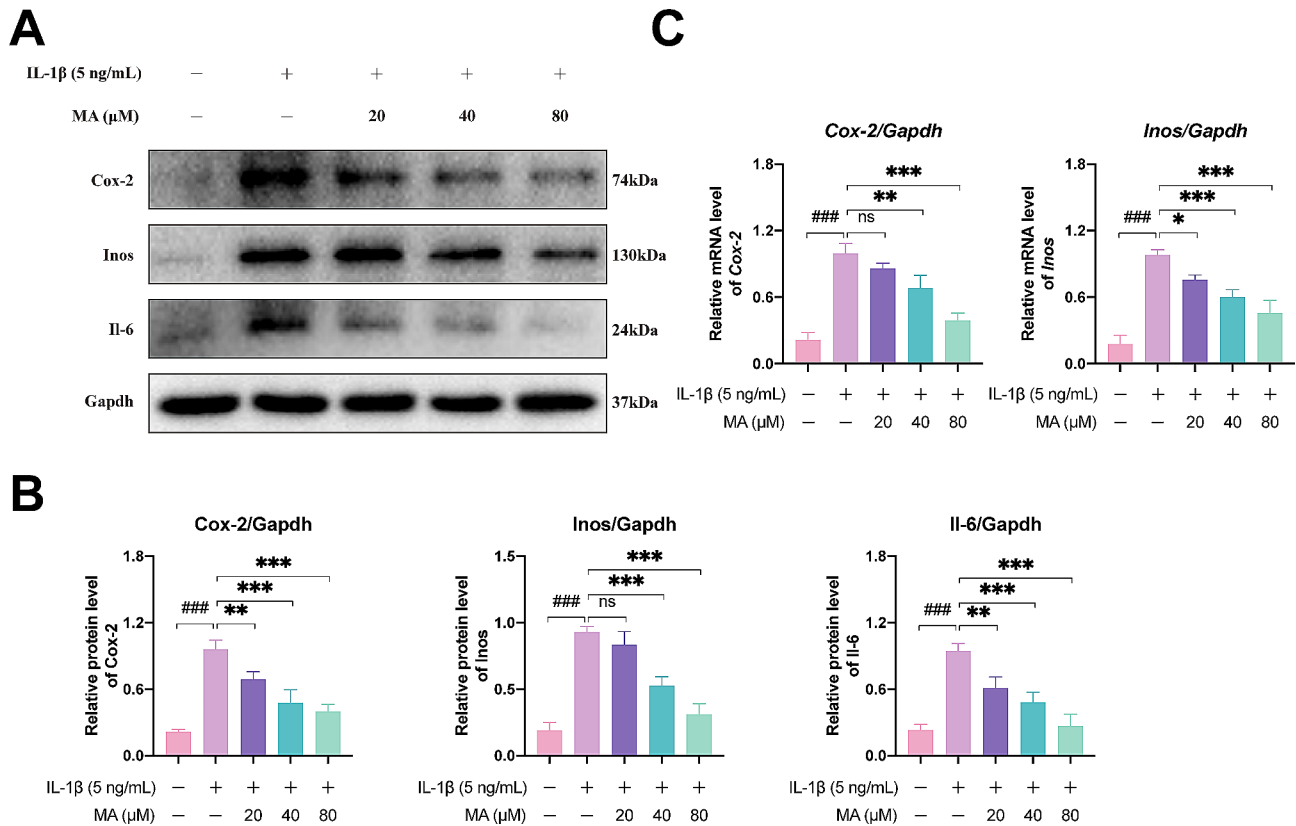


**Fig. 3** MA reduced the inflammation responses in IL-1β-stimulated NPCs. **(A-B)** The inflammatory proteins expressions (Inos, Cox-2, and IL-6) in NPCs shown in western blotting. **(C)** The mRNA expression levels of inflammatory genes (Inos and Cox-2) were analyzed by RT-qPCR. Data were shown as means ± SD, *n* = 3. \**p* < 0.05; \*\**p* < 0.01; \*\*\**p* < 0.001; ns, no significant difference

**MA inhibited activation of MAPK and NF-κB pathways in IL-1β-induced NPCs**

Activation of MAPK and NF-κB pathways contribute to the inflammation responses and the ECM degeneration in NPCs, while inhibition of the above two pathways can alleviate the progression of IVDD [9, 10]. A previous study showed that the above two pathways were a kind of early activation pathways, and the activation peaks at 15 min after IL-1β (5 ng/ml) stimulation [21]. To investigate the effect of MA on the two pathways, NPCs were induced with IL-1β (5 ng/ml) for 15 min or/and MA (20, 40, and 80 μM) for 24 h.

As shown in Fig. 4A-B and E-F, the key nodes of the two signaling pathways such as phospho-P65 (p-P65), phospho-P38 (p-P38), phospho-Jnk (p-Jnk), and phospho-Erk (p-Erk) were significantly activated 15 min after IL-1β stimulation. Whereas, the activation of these pathways was inhibited by the administration of MA. In addition, the expression of p-P65 was accumulated in the nucleus after IL-1β stimulation, while MA inhibited this nuclear translocation of p-P65 (Fig. 4C-D).

**MA suppressed the ECM degeneration via activating Ppar-γ in IL-1β-induced NPCs**

Previous study found that peroxisome proliferator activated receptor γ (Ppar-γ) has shown excellent anti-inflammatory characteristics by suppressing NF-κB pathway [22], and the expression level of Ppar-γ is down-regulated in various diseases, such as osteoarthritis [23], rheumatoid arthritis [24], and colitis [25]. In Fig. 5A-B, the data showed that IL-1β inhibited the expression of Ppar-γ in NPCs compared to the control group. However, the administration of MA reversed the decreasing trend of Ppar-γ in IL-1β-induced NPCs. Thus, we hypothesized that Ppar-γ may play a role in the progression of IVDD, and investigated whether the anti-degeneration effects of MA were dependent on Ppar-γ. Next, we introduced the Ppar-γ antagonist GW9662 into our experiment. As shown in Fig. 5, Ppar-γ in the NPCs was inhibited by using 10 μM GW9662, and these NPCs were followed the application of IL-1β (5 ng/mL) and MA (80 μM). The study showed that the production of Ppar-γ was suppressed by GW9662. In additional, the inhibition of Ppar-γ significantly increased the production of IL-6, Inos, Cox-2, Mmp13, Collagen I and decreased the production of Collagen II in MA-treated NPCs (Fig. 5C-D).

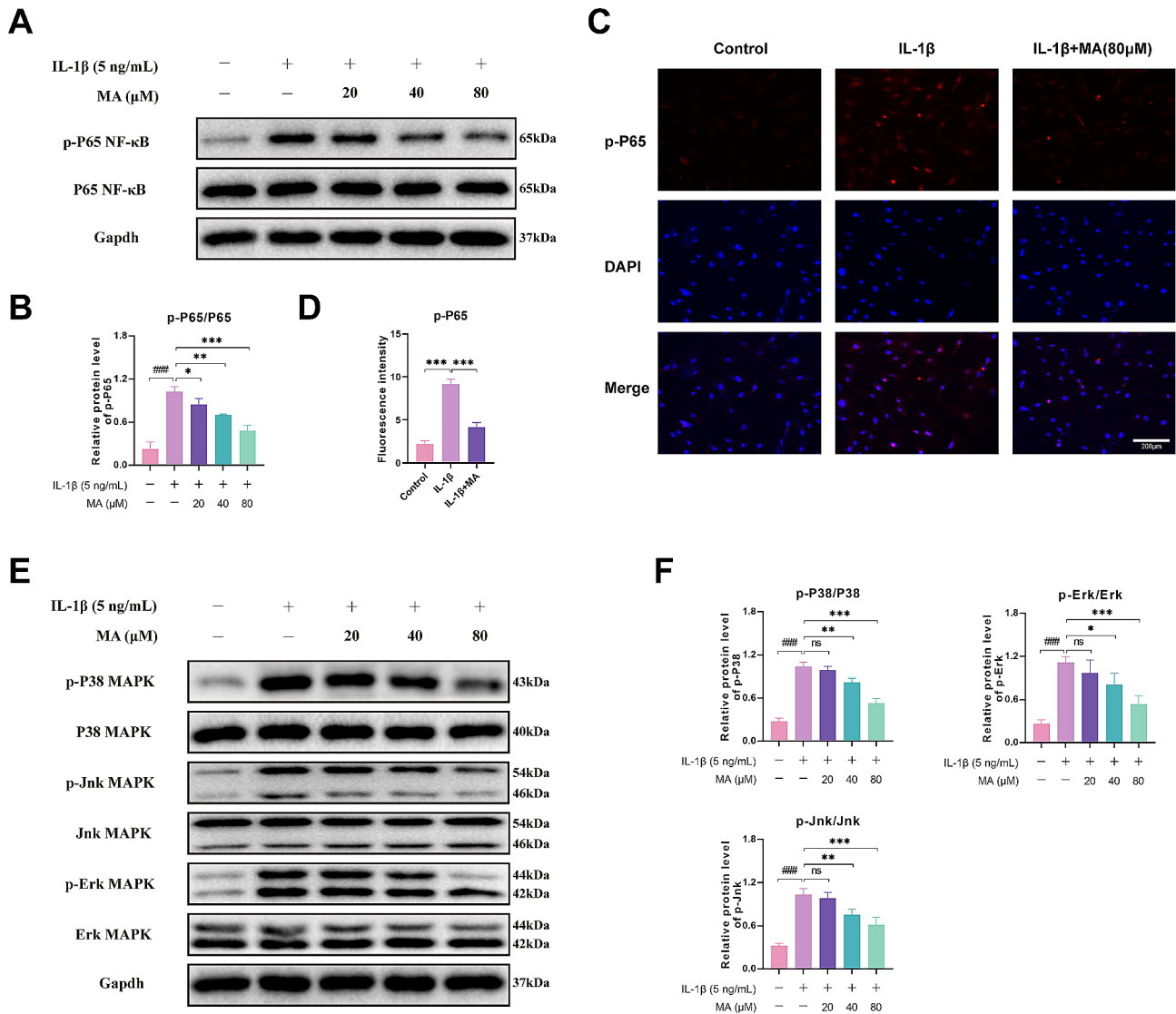


**Fig. 4** MA suppressed MAPK and NF-κB pathways in IL-1β-stimulated NPCs. The proteins expressions of NF-κB (P65) (A-B) and MAPK (P38, Jnk, and Erk) (E-F) were analyzed with western blotting. (C) Immunofluorescence staining and (D) quantitative analysis of the nuclear translocation of P-P65 in NPCs. Data were shown as means ± SD, n = 3. \*p < 0.05; \*\*p < 0.01; \*\*\*p < 0.001; ns, no significant difference

In addition, RT-qPCR detection confirmed the results shown by western blot (Fig. 5E). The above data suggested that MA inhibited the ECM degeneration in IL-1β-induced NPCs via activation of Ppar-γ.

**MA inhibited activation of NF-κB pathway via activating Ppar-γ in IL-1β-induced NPCs**

As shown above, IL-1β contributed to the activation of the MAPK and NF-κB pathways, which promoted the inflammatory response, enhanced ECM catabolism, suppressed ECM anabolism, and triggered ECM degeneration and development of IVDD. Conversely, MA blocked signaling transduction of the MAPK and NF-κB pathways. Furthermore, MA inhibited the ECM degeneration via activation of Ppar-γ in IL-1β-induced NPCs,

thus, we investigated whether MA ameliorated the ECM degeneration by inhibiting the two pathways via Ppar-γ. In Fig. 6, the data showed that the inhibition of Ppar-γ by the Ppar-γ antagonist GW9662 activated the NF-κB pathways in MA-treated NPCs, which suggested that MA might regulate the NF-κB signal via Ppar-γ. However, Ppar-γ antagonist GW9662 could not block the suppressive effect of MA on MAPK signaling.

**MA alleviated the progression of needle puncture-induced IVDD rat models**

In vivo, we designed to investigate the therapeutic effect of MA in rat models of IVDD. As shown in Fig. 7A-B, the X-ray and MRI images revealed the stenosis of the intervertebral space and the decreased T2-weighted signal

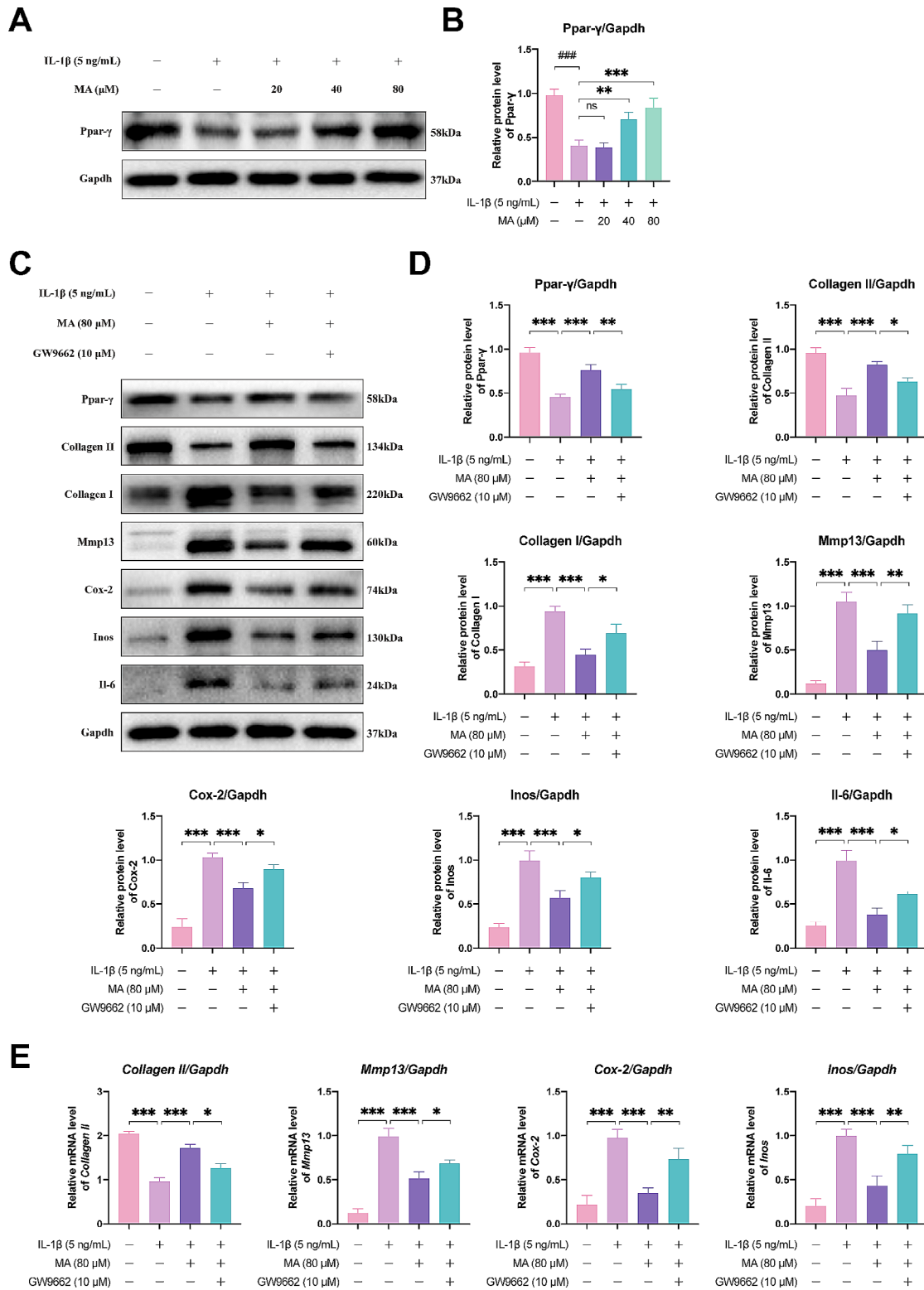


**Fig. 5** Inhibition of Ppar- $\gamma$  weakened the anti-inflammatory, anabolism enhancing, and catabolism suppressing effects of MA on IL-1 $\beta$ - stimulated NPCs. (A-B) The proteins expressions of Ppar- $\gamma$  were analyzed with western blotting. (C-D) The expressions of anabolic proteins (Collagen II and Collagen I) and catabolic protein (Mmp13) in the Ppar- $\gamma$ -inhibition NPCs along with or without the administration of 5 ng/ml of IL-1 $\beta$  and 80  $\mu$ M of MA. (E) The mRNA expression of Collagen II, Mmp13, Cox-2, and Inos were detected by RT-qPCR analysis. Data were shown as means  $\pm$  SD,  $n=3$ . \* $p<0.05$ ; \*\* $p<0.01$ ; \*\*\* $p<0.001$ ; ns, no significant difference

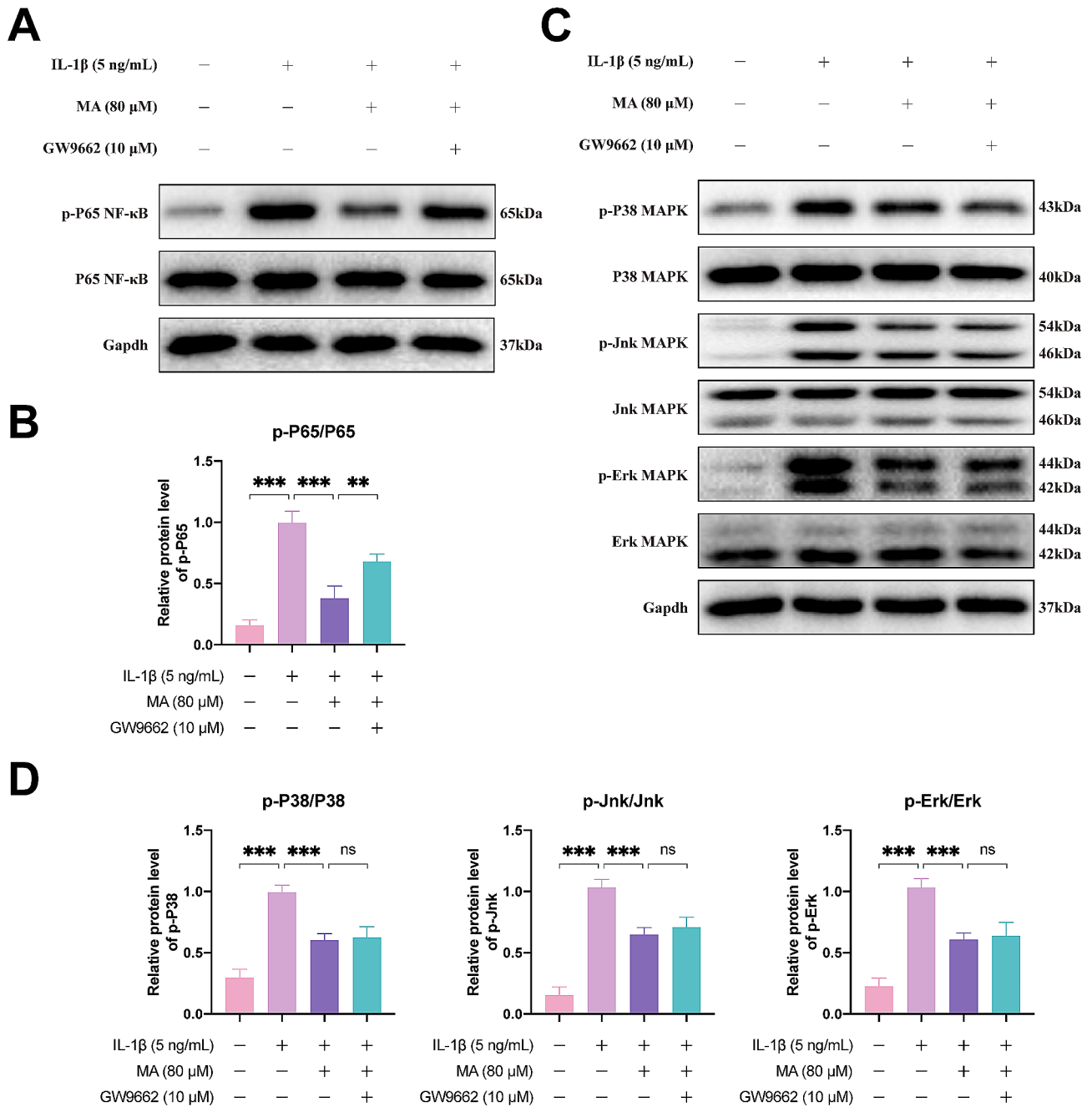


**Fig. 6** Inhibition of Ppar-γ weakened the inhibition effect of MA on NF-κB signaling pathway in IL-1β-stimulated NPCs. **(A-D)** Western blot analysis showed the inhibition of Ppar-γ activated the NF-κB (P65) and MAPK (P38, Jnk, and Erk) signaling pathway. Data were shown as means±SD, *n*=3. \**p*<0.05; \*\**p*<0.01; \*\*\**p*<0.001; ns, no significant difference

intensity after surgery. However, the above IVDD-like features were significantly reversed with the application of MA. Furthermore, disc specimens stained with H&E and Safranin O/Fast Green revealed significant morphological changes in the IVDD group, whereas the trend of deterioration was alleviated after the MA treatment in the IVDD+MA group (Fig. 7C-D). Additionally, the IVDD+MA group showed a remarkable recovery of ECM compared to the IVDD group. As in the IVDD

group, the production of Mmp13 was upregulated, together with the decreased of Collagen II and Aggrecan; however, in the IVDD+MA group, the production of Mmp13, Collagen II, and Aggrecan were reversed after MA treatment (Fig. 7E-F). In addition, the expression of Ppar-γ was downregulated in the IVDD group compared to the SHAM group, whereas the IVDD+MA group showed an upregulation of Ppar-γ after the MA treatment (Fig. 7E-F). Taken together, the above in vivo results

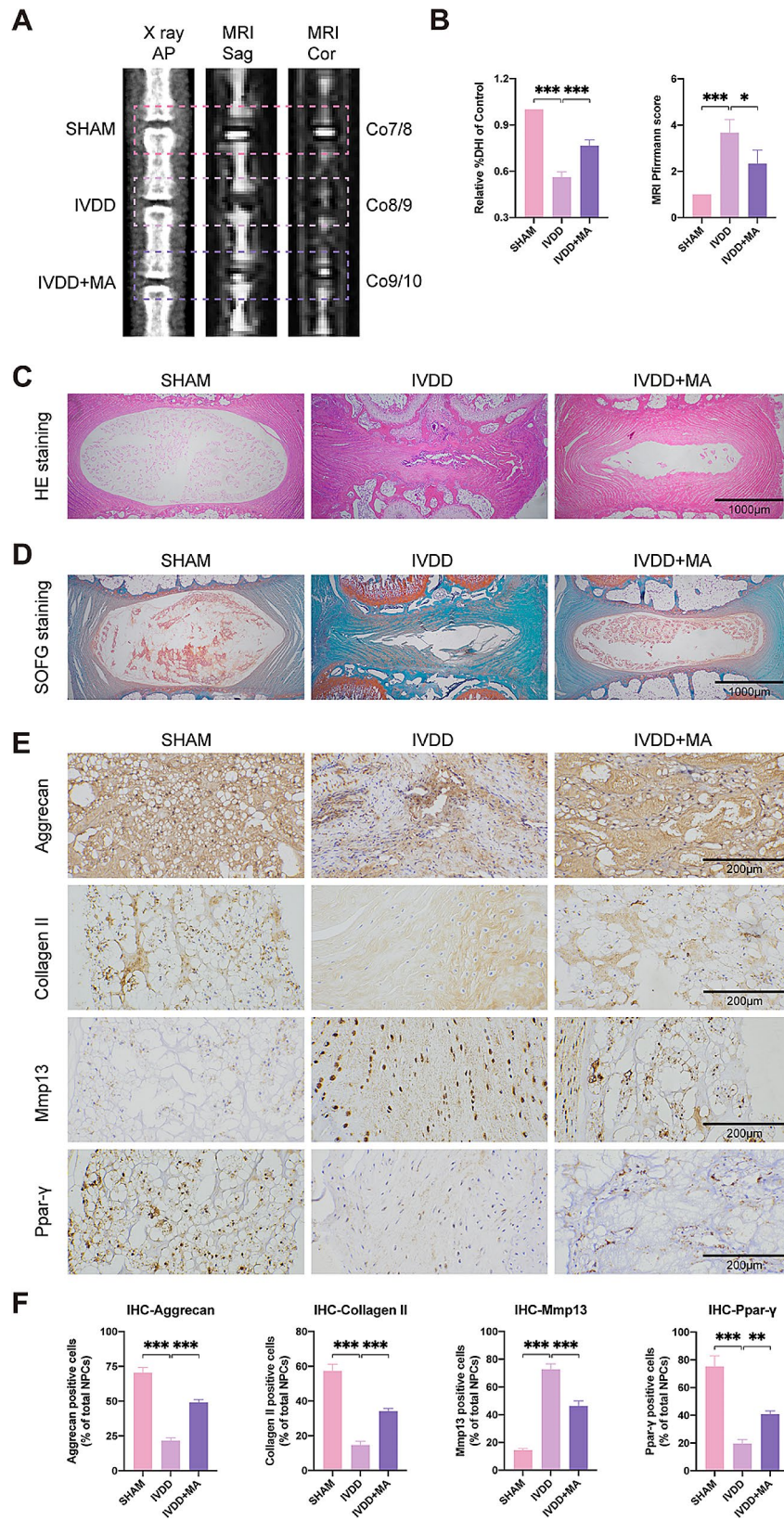


**Fig. 7** MA ameliorated IVDD-related change in rat IVDD models. **(A)** The representative X-ray images and MRI images **(B)** the measurement of DHI and the evaluation of Pfirrmann score among the SHAM, IVDD, and IVDD + MA groups. **(C)** H&E staining, **(D)** Safranin O/Fast Green staining. **(E)** IHC images of Aggrecan, Mmp13, Collagen II, Ppar-γ, and **(F)** the quantification of positive NPCs. Data were shown as means ± SD, *n* = 6. \**p* < 0.05; \*\**p* < 0.01; \*\*\**p* < 0.001; ns, no significant difference

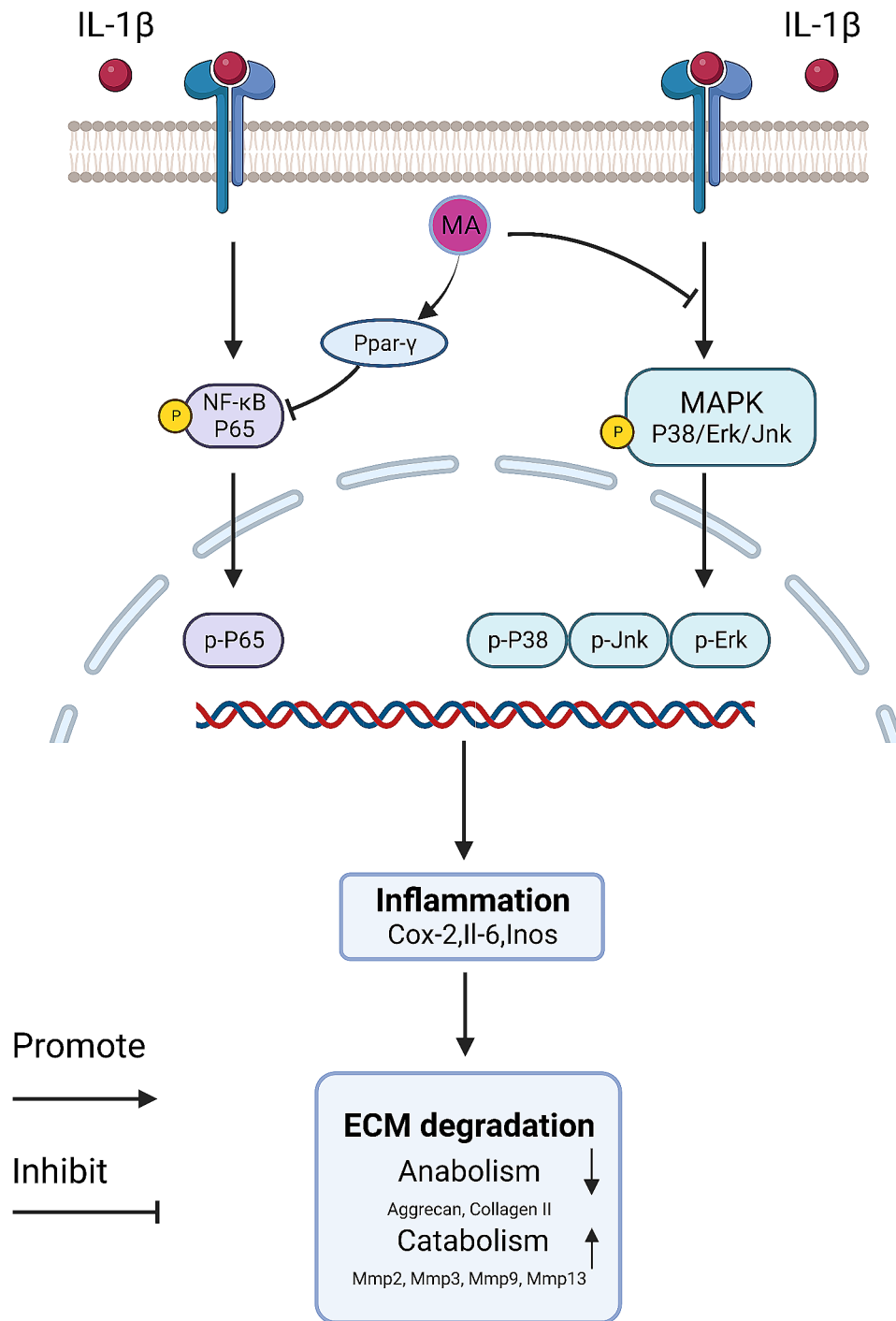


**Fig. 8** Schematic illustration of the potential protective effects of MA on the progression of IVDD (figure was created with <https://www.biorender.com/>). MA alleviates the progression of IVDD via the MAPK and Ppar-γ/NF-κB signaling pathways

demonstrated that MA treatment was effective in reversing degenerative phenotypes, thereby alleviating the progression of IVDD.

## Discussion

IVDD is the main cause of low back pain. It also causes the neurological damage, which affects the daily work and quality of life among the middle-aged workers and elderly people [26–28]. Current clinical strategies for IVDD mainly focus on the use of conventional drugs, which aim to alleviate symptoms, and most of them cannot reverse the pathological changes of IVDD. Therefore, it is necessary to explore a drug that not only allivates the symptoms, but also reverses the pathological change to delay the progression of IVDD. Previous studies have shown that inflammation may contribute to the progression of IVDD [7, 29]. MA, as a natural polyhydroxylated stilbene compound extracted from Mori cortex, has been reported to have a significant effect on anti-hyperuricemic, anti-inflammatory, anti-osteoarthritis, and anti-kidney cancer effects [14–16, 30]. According to our previous research, MA has anti-inflammatory effects on osteoarthritis [16]. However, the therapeutic role of MA in IVDD has not been investigated. This study is the first to show that MA has the property of alleviating IVDD, and this effect is based on the activation of PPAR- $\gamma$ .

The anabolic and catabolic phenotypes of NPCs play an important role in maintaining the metabolic homeostasis of the intervertebral disc microenvironment. IVDD is generally considered as a result of increased catabolism and decreased anabolism, as both types of metabolism trigger to the ECM degradation. Mmps, including Mmp2, Mmp3, Mmp9, and Mmp13, are crucial types of ECM catabolism proteins in NPCs [31]. Crean et al. reported that the increased expression of Mmp9 and Mmp2 was closely associated with the severe degree of IVDD [32]. In addition, Le Maitre et al. showed that the Mmp13 protein was significantly upregulated in the early degenerated inner of NPCs [33]. As another major component of the ECM in NPCs, Aggrecan and Collagen II are crucial for maintaining the osmotic pressure and resilience of the NPCs [34]. Our data showed that MA inhibited the production of Mmp13, Mmp9, and Mmp2, and promoted the production of Collagen II and Aggrecan in IL-1 $\beta$ -induced NPCs. Inflammatory proteins, including Inos, Cox-2, and Il-6, are correlated with the IVDD progression [29, 35, 36]. These inflammatory markers could further increase the catabolic-related proteins and decrease the anabolic-related proteins. Our study showed that MA application significantly IL-1 $\beta$ -pretreated NPCs. What's more, in vivo experiments showed that the administration of MA into acupuncture discs attenuated the progression of IVDD in rat models.

Inflammatory pathways, such as MAPK and NF- $\kappa$ B, are both key negative regulators on the catabolism and anabolism in NPCs and promote the progression of IVDD [9, 10]. Previous research has shown that the successful transmission of the above two signaling pathways increase the production of inflammatory cytokines and catabolic-related proteins and decrease the production of anabolic-related proteins [9, 10, 16, 37]. In other words, inhibition of the two pathways may be a therapeutic target for IVDD. Our study showed that IL-1 $\beta$  upregulated the production of p-P38, p-Erk, p-Jnk, and p-P65. However, the application of MA reversed the upregulation of these proteins in IL-1 $\beta$ -induced NPCs, reflecting the inhibitory role of MA on MAPK and NF- $\kappa$ B pathways and suggesting that MA ameliorated the IVDD progression by suppressing the two signaling pathways.

Ppar- $\gamma$  is a ligand-activated transcription factor closely associated with many inflammatory diseases [38–41]. A previous study showed that the overexpression of Ppar- $\gamma$  inhibited synovial inflammation in rheumatoid arthritis [42]. The activation of Ppar- $\gamma$  has the chondroprotective effects on the progression of osteoarthritis [43]. Pioglitazone is a highly selective Ppar- $\gamma$  agonist. Liu et al. found that pioglitazone inhibited the generation of inflammatory cytokines and maintained the expression of anabolic proteins in IL-17 induced NPCs [44]. Another study showed that DNA methyltransferase 3a promotes apoptosis and ECM degradation of NPCs by inhibiting the expression of Ppar- $\gamma$  [45]. These findings suggest that Ppar- $\gamma$  may be a therapeutic target for IVDD. Our results demonstrated that MA had the ability to increase the expression of Ppar- $\gamma$ , suggesting that MA could be used as a type of Ppar- $\gamma$  agonist. Furthermore, the anti-inflammatory effects of MA were suppressed to some extent after the administration of Ppar- $\gamma$  specific antagonist GW9662. Therefore, we concluded that MA exerts its anti-inflammatory effects by activating Ppar- $\gamma$ . We further investigated whether the Ppar- $\gamma$  inhibition affects the following processes, such as inflammatory response, ECM degradation, and MAPK and NF- $\kappa$ B signaling transduction. Our studies showed that the inhibition of Ppar- $\gamma$  by GW9662 suppressed the anti-inflammatory properties of MA in IL-1 $\beta$ -induced NPCs. Meanwhile, it reversed the catabolism-suppressing and anabolism-enhancing roles of MA in IL-1 $\beta$ -induced NPCs. Its strong anti-inflammatory effect may be due to inhibition of NF- $\kappa$ B signaling transduction pathway [46, 47]. On the one hand, Ppar- $\gamma$  can directly interact with NF- $\kappa$ B p50/NF- $\kappa$ B p65 dimer to inhibit this nuclear translocation of p-P65. On the other hand, Ppar- $\gamma$  can inhibit I $\kappa$ B $\alpha$  degradation to inhibit NF- $\kappa$ B signaling [48]. In this study, we found that blocked Ppar- $\gamma$  impaired the suppressive effect of MA on the NF- $\kappa$ B signaling transduction. However, the inhibition of Ppar- $\gamma$  could not reverse the inhibitory

effect of MA on MAPK pathway. Previous research demonstrated that Jnk and P38 phosphorylate the amino-terminal domain of Ppar- $\gamma$  and subsequently decreased the production of Ppar- $\gamma$  [49], which is consistent with our experimental results. These above data suggested that the inflammatory inhibition role of MA in IL-1 $\beta$ -induced NPCs may be mediated via Ppar- $\gamma$ .

This study has several potential shortcomings. First, it is difficult to intervene directly and non-invasively the intervertebral disc, and target-NPCs drug delivery systems remain unexplored. Second, the anti-degenerative effect of MA on IVDD has not been verified on IVDD patients. Thus, the clinical effects of MA on IVDD patients need to be further investigated. Third, the conclusion of this study was that MA played a role in ameliorating IVDD by inhibiting the MAPK and Ppar- $\gamma$ /NF- $\kappa$ B signaling pathways, but this may not be the only mechanism of MA on NPCs. Forth, the underlying mechanism is demonstrated only in vitro and requires further in vivo validation. Fifth, our study showed that MA inhibits IVDD by activating the expression of Ppar- $\gamma$ , but its therapeutic efficacy lacks comparison with pioglitazone, a commonly used Ppar- $\gamma$  agonist. In the future, we will explore the potential mechanisms of MA in more depth and compare the therapeutic efficacy with other drugs for IVDD treatment. Considering the potential therapeutic effect of MA on IVDD in rat, further study remains to be performed.

## Conclusion

As shown in Fig. 8, our study is the first to demonstrated that MA treatment has anti-inflammatory properties by suppressing the MAPK and NF- $\kappa$ B pathways in rat models. The protective mechanism of MA on IVDD is closely related to the activation of Ppar- $\gamma$ , suggesting that MA or Ppar- $\gamma$  may be a potential drug or molecular target for the treatment of IVDD.

## Abbreviations

IVDD	Intervertebral disc degeneration
MA	Mulberroside A
ECM	Extracellular matrix
MAPK	Mitogen-activated protein kinase
NF- $\kappa$ B	Nuclear factor kappa-B
NPCs	Nucleus pulposus cells
Mmps	Matrix metalloproteinases
p-P65	Phosphor-P65
p-P38	Phospho-P38
p-Jnk	Phosphor-Jnk
p-Erk	Phosphor-Erk
Ppar- $\gamma$	Peroxisome proliferator activated receptor

## Supplementary Information

The online version contains supplementary material available at <https://doi.org/10.1186/s12950-024-00398-7>.

Supplementary Material 1

## Acknowledgements

Not Applicable.

## Author contributions

Conceptualization: Tao Xu, Rui Lu, Hua Wu; Data curation: Tao Xu, Hongqi Zhao, Xuan Fang, Shanxi Wang, Jian Li, Hua Wu, Rui Lu; Formal analysis: Hongqi Zhao, Xuan Fang; Funding acquisition: Rui Lu, Hua Wu, and Weihua Hu; Methodology: Tao Xu, Weihua Hu, Shanxi Wang, Jian Li; Project administration: Hongqi Zhao and Rui Lu; Software: Shanxi Wang, Jian Li; Supervision: Hua Wu, Weihua Hu, Rui Lu; Validation: Weihua Hu, Hongqi Zhao, Xuan Fang, Shanxi Wang, Jian Li; Visualization: Xuan Fang, Shanxi Wang; Writing – original draft: Tao Xu, Hongqi Zhao; Writing – review & editing: Tao Xu, Weihua Hu, and Rui Lu. All authors reviewed the manuscript.

## Funding

This research was supported by the National Natural Science Foundation of China (Grant No. 51877097), Project Fund for Outstanding Doctoral Talents in Zhongnan Hospital of Wuhan University (Grant No. ZNYB2023008), Hubei Provincial Natural Science Foundation of China (Grant No. 2023AFB646), Knowledge Innovation Program of Wuhan-Basic Research (Grant No. 2023020201010155), and Educational Research Program of Huazhong University of Science and Technology (Grant No. 2022135).

## Data availability

Data is provided within the manuscript or supplementary information files.

## Declarations

### Ethics approval and consent to participate

The study was approved by the Ethics Committee on Animal Experimentation of Tongji Hospital, Tongji Medical College, Huazhong University of Science and Technology.

### Consent for publication

Not Applicable.

### Competing interests

The authors declare no competing interests.

### Conflict of interest

The authors declare that the research was conducted in the absence of any commercial or financial relationships that could be construed as a potential conflict of interest.

Received: 12 March 2024 / Accepted: 12 June 2024

Published online: 28 August 2024

## References

1. Cieza A, Causey K, Kamenov K, Hanson SW, Chatterji S, Vos T. Global estimates of the need for rehabilitation based on the Global Burden of Disease Study 2019: a systematic analysis for the global burden of Disease Study 2019. *Lancet*. 2021;396:2006–17. [https://doi.org/10.1016/S0140-6736\(20\)32340-0](https://doi.org/10.1016/S0140-6736(20)32340-0).
2. Driscoll T, Jacklyn G, Orchard J, Passmore E, Vos T, Freedman G, et al. The global burden of occupationally related low back pain: estimates from the global burden of Disease 2010 study. *Ann Rheum Dis*. 2014;73:975–81. <https://doi.org/10.1136/annrheumdis-2013-204631>.
3. Mohd Isa IL, Teoh SL, Nor M, N. H., and, Mokhtar SA. Discogenic low back Pain: anatomy, pathophysiology and treatments of intervertebral disc degeneration. *Int J Mol Sci*. 2022;24. <https://doi.org/10.3390/ijms24010208>.
4. Desmoulin GT, Pradhan V, Milner TE. Mechanical aspects of intervertebral disc Injury and implications on Biomechanics. *Spine*. 2020;45:E457–64. <https://doi.org/10.1097/BRS.0000000000003291>.
5. Mayer JE, Iatridis JC, Chan D, Qureshi SA, Gottesman O, Hecht AC. Genetic polymorphisms associated with intervertebral disc degeneration. *Spine J*. 2013;13:299–317. <https://doi.org/10.1016/j.spinee.2013.01.041>.
6. Vieira LA, Dos Santos AA, Peluso C, Barbosa CP, Bianco B, Rodrigues L. Influence of lifestyle characteristics and VDR polymorphisms as risk factors for intervertebral disc degeneration: a case-control study. *Eur J Med Res*. 2018;23:11. <https://doi.org/10.1186/s40001-018-0309-x>.

7. Wang Y, Che M, Xin J, Zheng Z, Li J, Zhang S. The role of IL-1 $\beta$  and TNF- $\alpha$  in intervertebral disc degeneration. *Biomed Pharmacother*. 2020;131:110660. <https://doi.org/10.1016/j.biopha.2020.110660>.
8. Zhao K, An R, Xiang Q, Li G, Wang K, Song Y, et al. Acid-sensing ion channels regulate nucleus pulposus cell inflammation and pyroptosis via the NLRP3 inflammasome in intervertebral disc degeneration. *Cell Prolif*. 2021;54:e12941. <https://doi.org/10.1111/cpr.12941>.
9. Zhang GZ, Liu MQ, Chen HW, Wu ZL, Gao YC, Ma ZJ, et al. NF- $\kappa$ B signalling pathways in nucleus pulposus cell function and intervertebral disc degeneration. *Cell Prolif*. 2021;54:e13057. <https://doi.org/10.1111/cpr.13057>.
10. Zhang HJ, Liao HY, Bai DY, Wang ZQ, Xie XW. MAPK/ERK signaling pathway: a potential target for the treatment of intervertebral disc degeneration. *Biomed Pharmacotherapy = Biomedecine Pharmacotherapie*. 2021;143:112170. <https://doi.org/10.1016/j.biopha.2021.112170>.
11. Hu X, Zhang K, Pan G, Wang Y, Shen Y, Peng C, et al. Cortex Mori extracts induce apoptosis and inhibit tumor invasion via blockage of the PI3K/AKT signaling in melanoma cells. *Front Pharmacol*. 2022;13:1007279.
12. Ma LL, Yuan YY, Zhao M, Zhou XR, Jehangir T, Wang FY, et al. Mori Cortex extract ameliorates nonalcoholic fatty liver disease (NAFLD) and insulin resistance in high-fat-diet/streptozotocin-induced type 2 diabetes in rats. *Chin J Nat Med*. 2018;16(6):411–7.
13. Wang CP, Zhang LZ, Li GC, Shi YW, Li JL, Zhang XC, et al. Mulberoside A protects against ischemic impairment in primary culture of rat cortical neurons after oxygen-glucose deprivation followed by reperfusion. *J Neurosci Res*. 2014;92:944–54. <https://doi.org/10.1002/jnr.23374>.
14. Wang CP, Wang Y, Wang X, Zhang X, Ye JF, Hu LS, et al. Mulberoside A possesses potent uricosuric and nephroprotective effects in hyperuricemic mice. *Planta Med*. 2011;77:786–94. <https://doi.org/10.1055/s-0030-1250599>.
15. Zhang Z, Shi L. Anti-inflammatory and analgesic properties of cis-mulberoside A from *Ramulus mori*. *Fitoterapia*. 2010;81:214–8. <https://doi.org/10.1016/j.fitote.2009.09.005>.
16. Lu R, Wei Z, Wang Z, Xu S, Sun K, Cheng P, et al. Mulberoside A alleviates osteoarthritis via restoring impaired autophagy and suppressing MAPK/NF- $\kappa$ B/PI3K-AKT-mTOR signaling pathways. *iScience*. 2023;26:105936. <https://doi.org/10.1016/j.isci.2023.105936>.
17. Mosley GE, Hoy RC, Nasser P, Kaseta T, Lai A, Evashwick-Rogler TW, et al. Sex differences in rat intervertebral disc structure and function following annular puncture. *Injury*. 2019;44:1257–69. <https://doi.org/10.1097/BRS.0000000000003055>.
18. Vergroesen PP, Kingma I, Emanuel KS, Hoogendoorn RJ, Welting TJ, van Royen BJ, et al. Mechanics and biology in intervertebral disc degeneration: a vicious circle. *Osteoarthritis Cartil*. 2015;23:1057–70. <https://doi.org/10.1016/j.joca.2015.03.028>.
19. Wu X, Liu Y, Guo X, Zhou W, Wang L, Shi J, et al. Prolactin inhibits the progression of intervertebral disc degeneration through inactivation of the NF- $\kappa$ B pathway in rats. *Cell Death Dis*. 2018;9:98. <https://doi.org/10.1038/s41419-017-0151-z>.
20. Pfirrmann CW, Metzendorf A, Zanetti M, Hodler J, Boos N. Magnetic resonance classification of lumbar intervertebral disc degeneration. *Spine*. 2001;26:1873–8. <https://doi.org/10.1097/00007632-200109010-00011>.
21. Lu R, Xu H, Deng X, Wang Y, He Z, Xu S, et al. Physalin A alleviates intervertebral disc degeneration via anti-inflammatory and anti-fibrotic effects. *J Orthop Translat*. 2023;39:74–87. <https://doi.org/10.1016/j.jot.2023.01.001>.
22. Li H, Ooi SQ, Heng CK. The role of NF- $\kappa$ B in SAA-induced peroxisome proliferator-activated receptor  $\gamma$  activation. *Atherosclerosis*. 2013;227:72–8. <https://doi.org/10.1016/j.atherosclerosis.2012.12.007>.
23. Nebbaki SS, Mansouri E, Afif FE, Kapoor H, Benderdour M, Duval M, N., et al. Egr-1 contributes to IL-1-mediated down-regulation of peroxisome proliferator-activated receptor  $\gamma$  expression in human osteoarthritic chondrocytes. *Arthritis Res Ther*. 2012;14:R69. <https://doi.org/10.1186/ar3788>.
24. Marder W, Khalatbari S, Myles JD, Hench R, Lustig S, Yalavarthi S, et al. The peroxisome proliferator activated receptor- $\gamma$  pioglitazone improves vascular function and decreases disease activity in patients with rheumatoid arthritis. *J Am Heart Assoc*. 2013;2:e000441. <https://doi.org/10.1161/JAHA.113.000441>.
25. Speca S, Dubuquoy L, Desreumaux P. Peroxisome proliferator-activated receptor gamma in the colon: inflammation and innate antimicrobial immunity. *J Clin Gastroenterol*. 2014;48(Suppl 1):S23–27. <https://doi.org/10.1097/MCG.0000000000000253>.
26. Sun Z, Liu ZH, Chen YF, Zhang YZ, Wan ZY, Zhang WL, et al. Molecular immunotherapy might shed a light on the treatment strategies for disc degeneration and herniation. *Med Hypotheses*. 2013;81:477–80. <https://doi.org/10.1016/j.mehy.2013.06.014>.
27. Wang F, Cai F, Shi R, Wang XH, Wu XT. Aging and age related stresses: a senescence mechanism of intervertebral disc degeneration. *Osteoarthritis Cartil*. 2016;24:398–408. <https://doi.org/10.1016/j.joca.2015.09.019>.
28. Williams RJ, Tryfonidou MA, Snuggs JW, Le Maitre CL. Cell sources proposed for nucleus pulposus regeneration. *JOR Spine*. 2021;4:e1175. <https://doi.org/10.1002/jsp2.1175>.
29. Khan AN, Jacobsen HE, Khan J, Filippi CG, Levine M, Lehman RA Jr, et al. Inflammatory biomarkers of low back pain and disc degeneration: a review. *Ann N Y Acad Sci*. 2017;1410:68–84. <https://doi.org/10.1111/nyas.13551>.
30. Duan C, Han J, Zhang C, Wu K, Lin Y. Inhibition of kidney cancer cell growth by Mulberoside-A is mediated via mitochondrial mediated apoptosis, inhibition of cell migration and invasion and targeting EGFR signalling pathway. *J B U : Official J Balkan Union Oncol*. 2019;24:296–300.
31. Vo NV, Hartman RA, Yurube T, Jacobs LJ, Sowa GA, Kang JD. Expression and regulation of metalloproteinases and their inhibitors in intervertebral disc aging and degeneration. *Spine J*. 2013;13:331–41. <https://doi.org/10.1016/j.spinee.2012.02.027>.
32. Crean JK, Roberts S, Jaffray DC, Eisenstein SM, Duance VC. Matrix metalloproteinases in the human intervertebral disc: role in disc degeneration and scoliosis. *Spine*. 1997;22:2877–84. <https://doi.org/10.1097/00007632-199712150-00010>.
33. Le Maitre CL, Freemont AJ, Hoyland JA. Localization of degradative enzymes and their inhibitors in the degenerate human intervertebral disc. *J Pathol*. 2004;204:47–54. <https://doi.org/10.1002/path.1608>.
34. Xu X, Wang D, Zheng C, Gao B, Fan J, Cheng P, et al. Progerin accumulation in nucleus pulposus cells impairs mitochondrial function and induces intervertebral disc degeneration and therapeutic effects of sulforaphane. *Theranostics*. 2019;9:2252–67. <https://doi.org/10.7150/thno.30658>.
35. Weber KT, Alipui DO, Sison CP, Bloom O, Quraishi S, Overby MC, et al. Serum levels of the proinflammatory cytokine interleukin-6 vary based on diagnoses in individuals with lumbar intervertebral disc diseases. *Arthritis Res Ther*. 2016;18:3. <https://doi.org/10.1186/s13075-015-0887-8>.
36. Zhao CQ, Zhang YH, Jiang SD, Li H, Jiang LS, Dai LY. ADAMTS-5 and intervertebral disc degeneration: the results of tissue immunohistochemistry and in vitro cell culture. *J Orthop Res*. 2011;29:718–25. <https://doi.org/10.1002/jor.21285>.
37. Shao Z, Wang B, Shi Y, Xie C, Huang C, Chen B, et al. Senolytic agent Quercetin ameliorates intervertebral disc degeneration via the Nrf2/NF- $\kappa$ B axis. *Osteoarthritis Cartil*. 2021;29:413–22. <https://doi.org/10.1016/j.joca.2020.11.006>.
38. Abdelrahman M, Sivarajah A, Thiernemann C. Beneficial effects of PPAR- $\gamma$  ligands in ischemia-reperfusion injury, inflammation and shock. *Cardiovasc Res*. 2005;65:772–81. <https://doi.org/10.1016/j.cardiores.2004.12.008>.
39. Giaginis C, Giagini A, Theocharis S. Peroxisome proliferator-activated receptor- $\gamma$  (PPAR- $\gamma$ ) ligands as potential therapeutic agents to treat arthritis. *Pharmacol Res*. 2009;60:160–9. <https://doi.org/10.1016/j.phrs.2009.02.005>.
40. Huang G, Jiang W, Xie W, Lu W, Zhu W, Deng Z. Role of peroxisome proliferator-activated receptors in osteoarthritis (review). *Mol Med Rep*. 2021;23. <https://doi.org/10.3892/mmr.2020.11798>.
41. Vetuschi A, Pompili S, Gaudio E, Latella G, Sferra R. PPAR- $\gamma$  with its anti-inflammatory and anti-fibrotic action could be an effective therapeutic target in IBD. *Eur Rev Med Pharmacol Sci*. 2018;22:8839–48. [https://doi.org/10.26355/eurrev\\_201812\\_16652](https://doi.org/10.26355/eurrev_201812_16652).
42. Li XF, Yin SQ, Li H, Yang YL, Chen X, Song B, et al. PPAR- $\gamma$  alleviates the inflammatory response in TNF- $\alpha$ -induced fibroblast-like synoviocytes by binding to p53 in rheumatoid arthritis. *Acta Pharmacol Sin*. 2023;44:454–64. <https://doi.org/10.1038/s41401-022-00957-9>.
43. Sheng W, Wang Q, Qin H, Cao S, Wei Y, Weng J, et al. Osteoarthritis: role of peroxisome proliferator-activated receptors. *Int J Mol Sci*. 2023;24(17):13137.
44. Liu Y, Qu Y, Liu L, Zhao H, Ma H, Si M, et al. PPAR- $\gamma$  agonist pioglitazone protects against IL-17 induced intervertebral disc inflammation and degeneration via suppression of NF- $\kappa$ B signaling pathway. *Int Immunopharmacol*. 2019;72:138–47. <https://doi.org/10.1016/j.intimp.2019.04.012>.
45. Cheng P, Wei HZ, Chen HW, Wang ZQ, Mao P, Zhang HH. DNMT3a-mediated methylation of PPAR $\gamma$  promote intervertebral disc degeneration by regulating the NF- $\kappa$ B pathway. *J Cell Mol Med*. 2024;28(2):e18048.
46. Marcone S, Haughton K, Simpson PJ, Belton O, Fitzgerald DJ. Milk-derived bioactive peptides inhibit human endothelial-monocyte interactions via PPAR- $\gamma$  dependent regulation of NF- $\kappa$ B. *J Inflamm (Lond)*. 2015;12(1):1.
47. Zhao Y, Li Z, Lu E, Sheng Q, Zhao Y. Berberine exerts neuroprotective activities against cerebral ischemia/reperfusion injury through up-regulating PPAR- $\gamma$  to suppress NF- $\kappa$ B-mediated pyroptosis. *Brain Res Bull*. 2021;177:22–30.

48. Zhu T, Zhang W, Feng SJ, Yu HP. Emodin suppresses LPS-induced inflammation in RAW264.7 cells through a PPAR $\gamma$ -dependent pathway. *Int Immunopharmacol.* 2016;34:16–24.
49. Yang Q, Chen C, Wu S, Zhang Y, Mao X, Wang W. Advanced glycation end products downregulates peroxisome proliferator-activated receptor  $\gamma$  expression in cultured rabbit chondrocyte through MAPK pathway. *Eur J Pharmacol.* 2010;649:108–14. <https://doi.org/10.1016/j.ejphar.2010.09.025>.

### **Publisher's Note**

Springer Nature remains neutral with regard to jurisdictional claims in published maps and institutional affiliations.